Effects of Crystal Phase Transformation on Tensile Properties of Polybutene-1/Cellulose Composites

Hisayuki Nakatani,[1] Yuuta Yamada,[1] Yuuta Takahashi,[1] Minoru Terano[2]

[1]*Department of Biotechnology and Environmental Chemistry, Kitami Institute of Technology 165 Koen-cho, Kitami, Hokkaido 090-8507, Japan*
[2]*School of Materials Science, Japan Advanced Institute of Science and Technology, 1-1 Asahidai, Nomi, Ishikawa 923-1292, Japan*

Received 7 January 2011; accepted 27 February 2011
DOI 10.1002/app.34423
Published online 25 July 2011 in Wiley Online Library (wileyonlinelibrary.com).

ABSTRACT: Morphologies and tensile properties of polybutene-1 (PB), PB/fibrous cellulose (FC), and the PB/silanized FC with 3-aminopropyltrimethoxysilane (APTMS) composites were studied. The scanning electron microscope micrographs exhibited the adherent PB parts on the FC and the silanized FC, suggesting that there was a certain affinity of PB to them. The spherulite observation suggested that there existed a secondary bonding between the PB and the FC or the silanized FC. These tensile properties were remarkably affected by the PB crystal phase transformation from the metastable tetragonal (II) to the stable hexagonal (I) phase. The transformation caused the ageing embrittlement even at r.t. In particular, the ageing embrittlement rate of the PB/silanized FC was much higher than other samples. Because the silanized FC became the excellent nucleating agent for the PB crystallization, the PB/silanized FC was found to easily form the thicker lamella having a higher probability of containing a crystal defect to serve as a starting point of the transformation. The higher transformation rate depended on the thicker lamella formation rate and its amount. © 2011 Wiley Periodicals, Inc. J Appl Polym Sci 123: 41–49, 2012

Key words: composites; crystallization; ductile; poly olefins; reinforcement

INTRODUCTION

Cellulose has been one of the most popular polymeric materials in the world and has been used as raw materials of building materials and paper for a long time ago. Cellulose is low cost, high modulus, renewable, and biodegradable. Recently, cellulose has attracted much attention as a composite material,[1–10] because it has great potential for the preparation of composite materials having high-modulus and renewability. As most popular composite based on cellulose, the composite with polyolefin has been extensively investigated by many resarchers.[1,3–13] In particular, polypropylene (PP) and polyethylene (PE) have been often used as the raw materials, and tensile properties and morphologies of their cellulose composites have been studied in detail. However, the cellulose composite with other polyolefin such as polybutene-1 (PB) has been little studied. Recently, Afrifah et al.[14] reported that the PB/cellulose composite showed processability, elongation at breaks, impact strength, and adhesion superior to those of the PP/- and PE/cellulose composites. These unique properties would be due to specific feature of PB.

PB is polymorphic and has mainly two kinds of crystalline form.[15–17] One is the stable hexagonal crystal form (I) with a characteristic peak at around 10° (2θ), the other is the metastable tetragonal one (II) with that at around 12° (2θ). It is well known that PB spontaneously exhibits a crystal phase transformation from II to I crystal forms.[15–17] In addition, it is well known that the transformation occurs during the PB plastic deformation and brings about a much more ductile behavior.[18] The good mechanical properties of the PB/cellulose must be originated from the crystal phase transformation. However, the effects of the crystal phase transformation on the mechanical properties such as tensile modulus have been not studied yet. In addition, it is known that PP/cellulose composite exhibits transcrystalline morphology under an isothermal crystallization condition.[19,20] The transcrystallization is ascribed to an interaction (secondary bonding) between cellulose and PP at a molecular level.[19] It seems that there exists such interaction in the PB/cellulose composite as well as PP one, and the interaction likely affects the behavior of the crystal phase transformation. However, the existence or nonexistence of the interaction has been not clarified yet.

The purpose of the present work has been to clarify the morphology and the tensile properties of the

Correspondence to: H. Nakatani (nakatani@chem.kitami-it.ac.jp).

PB/cellulose composite. In addition, the interaction between PB and cellulose has been investigated in comparison with a PB/silanized cellulose composite with APTMS. In this study, the behavior of the crystal phase transformation has been studied by wide-angle X-ray diffraction (WAXD) and differential scanning calorimetry (DSC) measurements. The morphologies and the tensile properties have been by polarizing microscope and scanning electron microscope (SEM) and by tensile testing, respectively.

EXPERIMENTAL

Materials

PB was supplied by Japan Polychem Co. The number–average molecular weight (M_n) and the polydispersity (M_w/M_n) were 1.0×10^5 and 5.2, respectively. The PB was reprecipitated from a boiling xylene solution into methanol and dried at 60°C for 8 h and was used as samples without antioxidant. FC (W-100GK) was donated by Nippon Paper Chemicals Co. The FC was dried in desiccator for 7 days before preparation. The moisture of the FC was below 0.7 wt %. The FC dimensions are over 90 wt % pass 100 mesh (below 150 μm), and the average length was ~ 37 μm. APTMS was purchased from Shinetsu Silicon Chemicals Co. and used without further purification.

Preparation of silanized FC

Mixing of 30 mL methanol solution of the APTMS silane coupling agent and the FC (1 g) were performed using a 0.1-L glass equipped with a stirrer at 23°C for 24 h. The methanol solvent was evaporated using a rotary evaporator. The samples obtained were dried at 60°C for 6 h at in a vacuum oven and were used as "silanized FC with APTMS."

Preparation of composites

Composites are prepared by an Imoto Seisakusyo IMC-1884 melting mixer. All mixtures were carried by each weight ratio. After a small amount of phenolic antioxidant (Adekastab AO-60, ~ 0.5%) was added, the mixing was performed at 150°C at 60 rpm for 5 min. The composites obtained were molded into the film (100 μm) by compression molding for 5 min at 150°C under 10 MPa and then was quickly quenched into a water bath. The film obtained was used as a "water quenched" sample.

Scanning electron microscope observation

Scanning electron microscope (SEM) observation was carried out with a JEOL JSM-5800 at 20 kV. The sample was fractured in liquid nitrogen and then was sputter-coated with gold.

Polarized optical microscope observation

Spherulite observations were carried out with a Nikon ECLIPSE 50/POL optical microscope (Nikon Corp. Tokyo, Japan) under nitrogen atmosphere. The isothermal crystallization temperature was controlled by a hot-stage system (Microscopy Hot-Stage, Imoto Seisakusyo, Kyoto, Japan). All samples were heated in the hot-stage and kept at 150°C for 5 min. They were quickly cooled to predetermined temperature and observed isothermally.

Tensile testing

Stress–strain behavior was observed using a SHIMADZU EZ-S at a cross-head speed of 3 mm/min. The sample specimens were cut with dimensions 30 × 5 × 0.1 mm shape in which the gauge length was 10 mm. We chose the specialized specimen (like ISO reed-shape) to adapt to the size of our tensile testing machine. All of tensile testing was performed at 20°C. The values of Young's modulus were obtained from the slope of the stress–strain curve (until about 1% of the strain value). All results obtained were the average values of 10 measurements.

Differential scanning calorimetry measurement

Differential scanning calorimetry (DSC) measurements were made with a Shimadzu DSC-60. The samples of about 2 mg weight were sealed in aluminum pans. The measurement of the samples was carried out at a heating rate of 10°C/min under nitrogen atmosphere.

Wide-angle X-ray diffraction measurement

Wide-angle X-ray diffraction (WAXD) diffractograms were recorded in reflection geometry at 2° (2θ/min) under Ni-filtered Cu Ka radiation using a RIGAKUXG-RINT 1200 diffractometer.

RESULTS AND DISCUSSION

Figure 1 shows the SEM micrographs of fractured surfaces of the water quenched PB/FC and PB/silanized FC with APTMS samples, respectively. In general, interfacial adhesion strength between polyolefin and cellulose is very poor because of each different polarity. However, as shown in Figure 1(a), the adherent PB on the FC can be observed (see the arrow). The SEM micrograph suggests that there is a certain affinity of PB to cellulose.[14] Figure 1(b) shows the interface of the PB/silanized FC. The

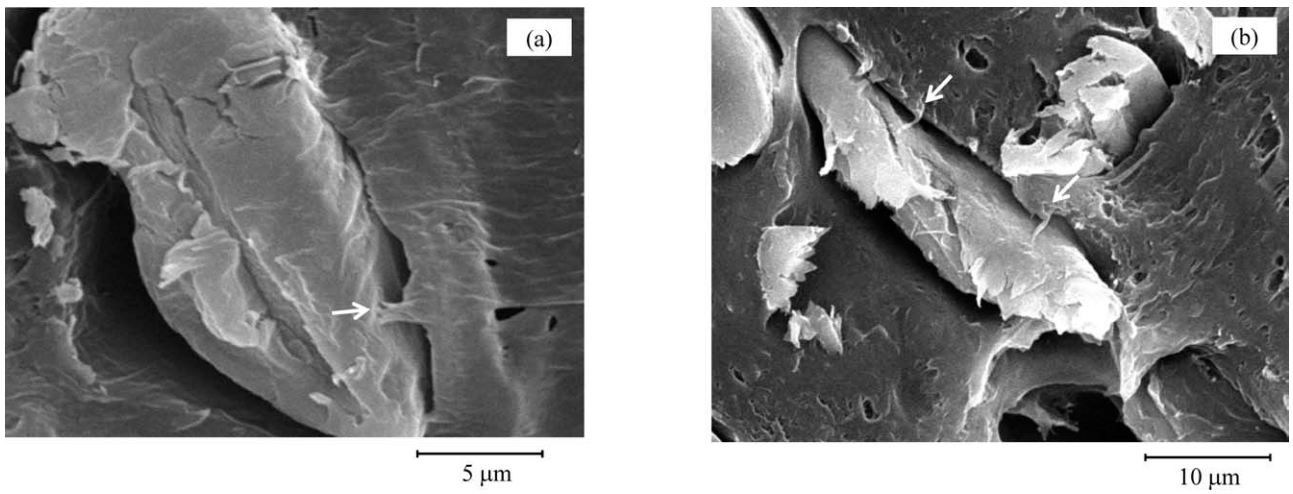

Figure 1 SEM microphotographs of the surfaces of the water quenched composite samples (aging time = 0 h). A: PB (70 wt %)/FC (30 wt %). B: PB (70 wt %)/silanized FC (30 wt %) with APTMS (5 wt %). The arrows indicate the adhesion PB.

adherent PB on the silanized FC can be observed as well as that of the PB/FC. Because there is no difference remarkable between these morphologies, it seems that the FC silanization hardly brings about the improvement of the interfacial adhesion. This behavior is considerably different from that of other polyolefin/FC composite.[21,22]

In general, PP/cellulose composite exhibits transcrystalline morphology under an isothermal or a slow cooling crystallization condition.[19,20,23,24] An adsorption configuration of a PP chain occurs by the interaction of a α-carbon/methyl moiety of PP and an oxygen in electron-rich glucosidic linkage in cellulose.[19] The adsorbed PP chain becomes a nuclear for transcrystallization at the cellulose surface, and the observation of the transcrystallization behavior has been often performed with the spherulite growth on the cellulose.[19,20,23,24] It seems that the adherent PB on the FC is due to the interaction as well as PP. To clarify the PB transcrystallization behavior on the FC, the PB spherulite growth was observed using the PB/FC and the PB/silanized FC. As shown in Figure 2(a), the spherulites growing on the FC can be observed. This result suggests that there exists the interaction between the PB and the FC surface. In the case PP/cellulose composite, a secondary bonding is created by the interaction between PP and cellulose. Unlike primary bonding, there is no transfer or sharing of electrons in secondary bonding. Therefore, the bonding force is much weaker,

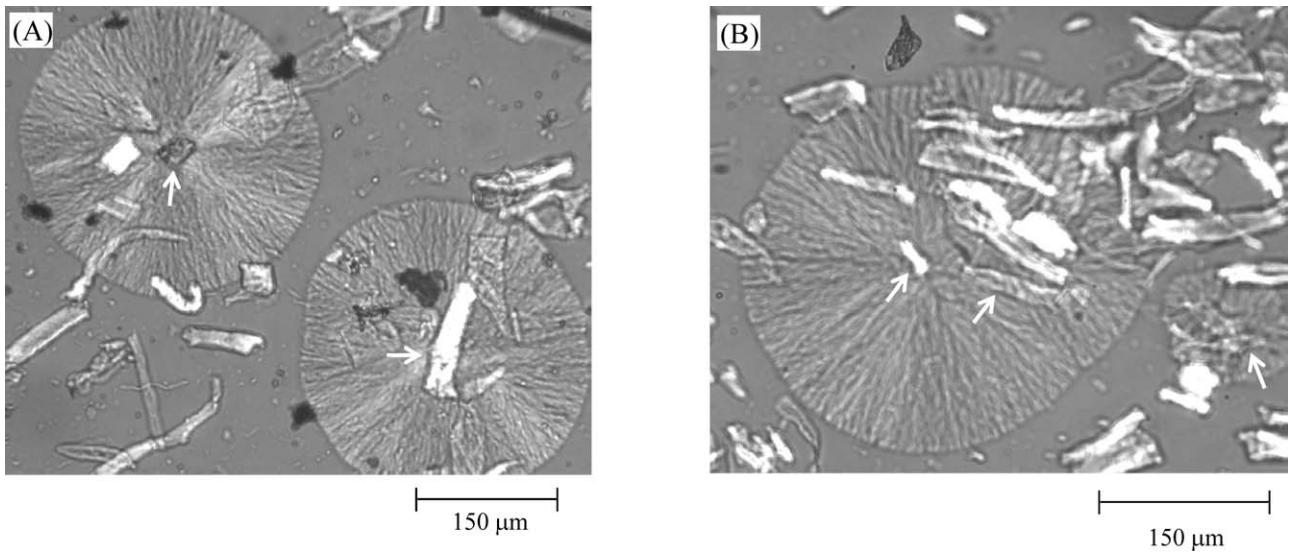

Figure 2 Optical micrographs of PB spherulites growing on the FC and the silanized FC at 95°C under nitrogen. A: PB (70 wt %)/FC (30 wt %). B: PB (70 wt %)/silanized FC (30 wt %) with APTMS (5 wt %). The arrows indicate the FC and the silanized FC, which are working as the nuclear agents. All samples are water-quenched composite samples (aging time = 0 h).

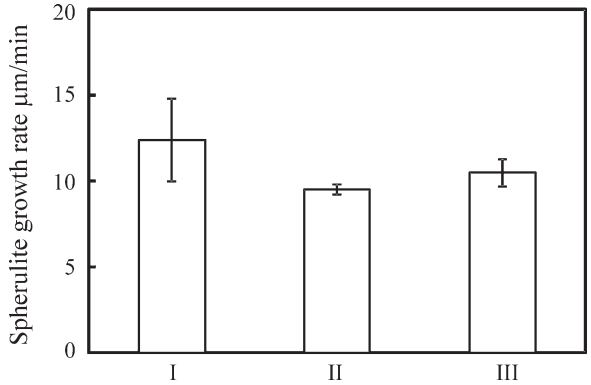

Figure 3 Comparisons of spherulite growth rates of samples at 95°C. I: PB. II: PB (70 wt %)/FC(30 wt %). III: PB (70 wt %)/silanized FC (30 wt %) with APTMS (5 wt %). The (II) and the (III) spherulite growth rates were obtained from the spherulites growing on the FC and the silanized FC. All samples are water-quenched composite samples (aging time = 0 h). All results obtained were the average values of five measurements.

and the appearance of the bonding hardly occurs except isothermal or slow cooling crystallization condition.[19,20,23,24] Before the bonding is formed, PP crystallization starts. In the case of PB, however, the crystallization rate is considerably slower than that of PP. Therefore, even under the water quenched condition, it seems that the secondary bonding is formed. The adherent PB, which is observed in Figure 1(a), is due to the formation of the secondary bonding. In addition, the secondary bonding can be also formed on the silanized FC with APTMS [see Figs. 1(b) and 2(b)]. There exists the amino group on the surface of the silanized FC.[22] The secondary bonding would be also able to be formed between the PB, and the silanized FC. Figure 3 shows the comparisons of spherulite growth rates of the PB, the PB on the FC, and the PB on the silanized FC. The spherulite growth rates of both the PBs on the FC and on the silanized FC are slightly lower than that of the PB. The lower rates also support that the PB transcrystallization processes occur in both the PB composite systems.

Figures 4–6 show the changes of the Young's moduli, the tensile strengths, and the elongation at breaks of the water quenched samples against the aging time at r.t. (~ 20°C). Although the tensile strength of the PB is almost constant against the aging time, the Young's modulus remarkably increases at the 168 h aging time, and the elongation

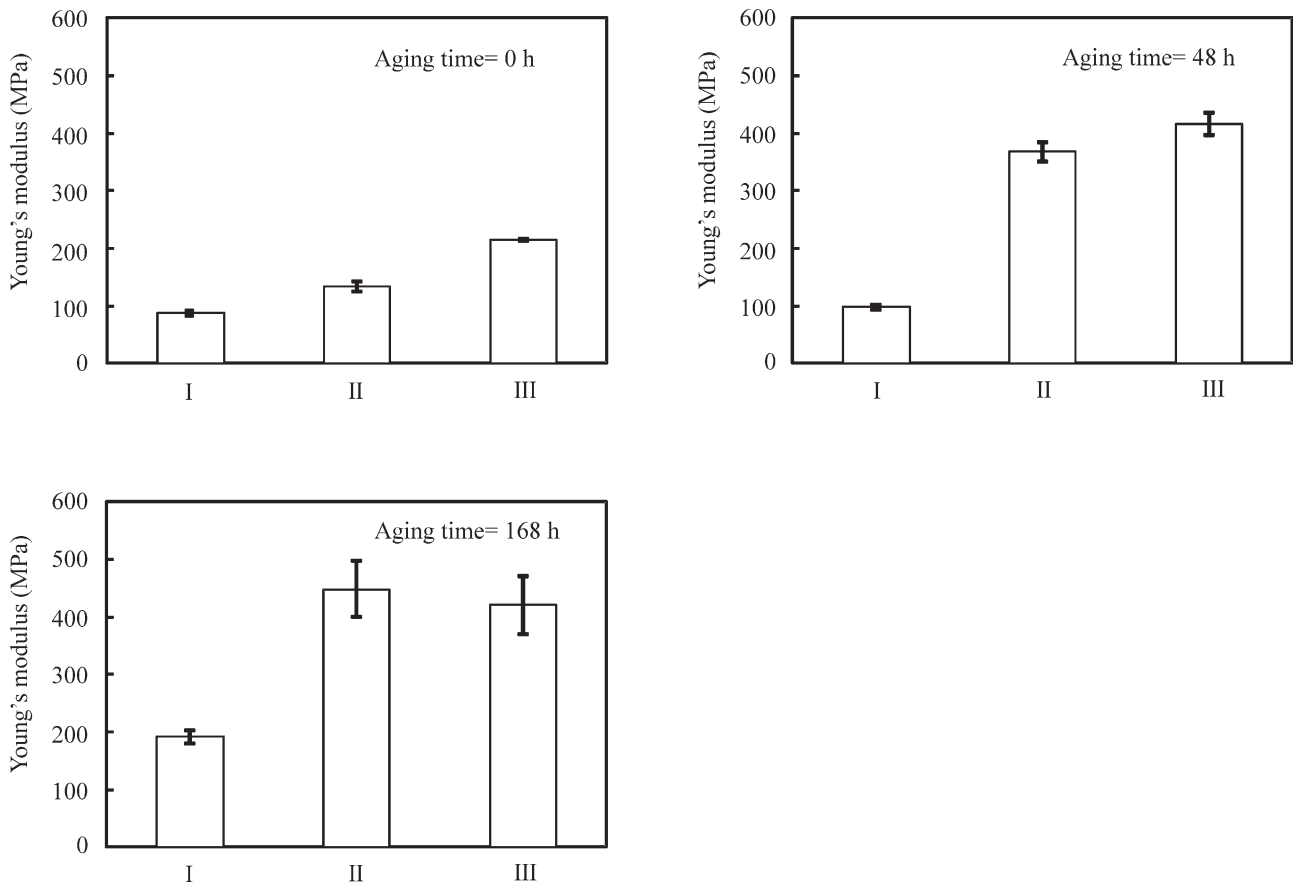

Figure 4 Comparison of Young's moduli of samples. I: PB. II: PB (70 wt %)/FC (30 wt %). III: PB (70 wt %)/silanized FC (30 wt %) with APTMS(5 wt %). Aging temperature = r. t. (~ 20°C).

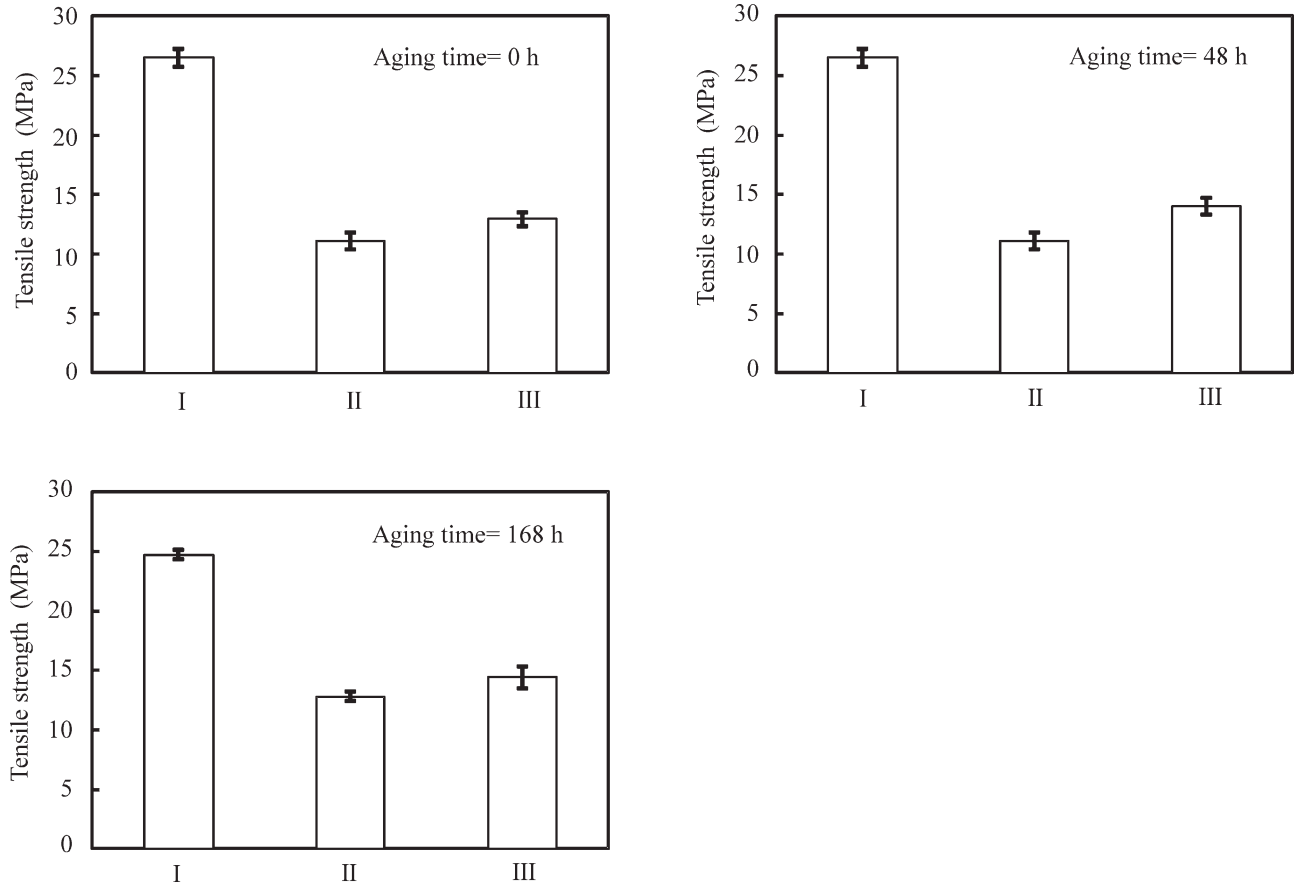

Figure 5 Comparison of tensile strengths of samples. I: PB. II: PB(70 wt %)/FC(30 wt %). III: PB(70 wt %)/silanized FC(30 wt %) with APTMS(5 wt %). Aging temperature = r. t. (~ 20°C).

at break remarkably decreases at the aging time. These changes of the PB tensile behavior indicate that an ageing embrittlement of the PB occurs. In the case of crystalline polymer, its ageing embrittlement is often originated from an increase of its crystallinity. However, the PB aging treatment has been performed at r.t., resulting that the increase of the crystallinity hardly occurs. The ageing embrittlement behavior must be due to the PB crystal phase transformation from the II to the I crystal form. It is well known that the transformation occurs during the PB plastic deformation and brings about a much more ductile behavior.[18] In fact, as shown in Figure 7, the crystalline part of the water-quenched PB is mainly composed of the I crystal form. The ductile behavior such as the lower Young's modulus and the longer elongation at break is originated from the applied energy absorption due to the crystal phase transformation. The existences of the FC and the silanized FC remarkably bring about the increases of the Young's moduli. The Young's moduli of these water quenched samples are ~ 150 and ~ 245% higher than that of the PB, respectively. Interestingly, the elongations at break of these water quenched samples are ~ 170%. These values are ~ 20 times higher than those of PP/FC and PP/silanized FC,[22] indicating that these PB composites are very ductile.[14] Because interface strength between polyolefin and FC is considerably weak, the origin of fracture is often its interface. However, in the cases of these PB composites, the applied stress is absorbed by the PB crystal phase transformation and would hardly concentrate on the interface. As shown in Figure 7, the crystalline parts of these water-quenched composites are mainly composed of the I crystal form as well as that of PB. The excellent ductile behavior of these PB composites is explainable in terms of the PB crystal phase transformation. The ageing embrittlements of these PB composites can also be observed. However, the ageing embrittlement rates of the PB/FC and the PB/silanized FC are higher than that of the PB. As shown in Figures 4–6, in particular, the changes of the PB/silanized FC tensile properties stopped at the 48-h aging time, suggesting that the ageing embrittlement rate is much higher than other samples.

Figure 8 shows the changes of the I/II peak intensity ratio of the PB, the PB/FC, and the PB/silanized FC with APTMS against the aging time at r.t. The I/II peak intensity ratio is obtained from the WAXD spectrum of each sample and can be used as a guide

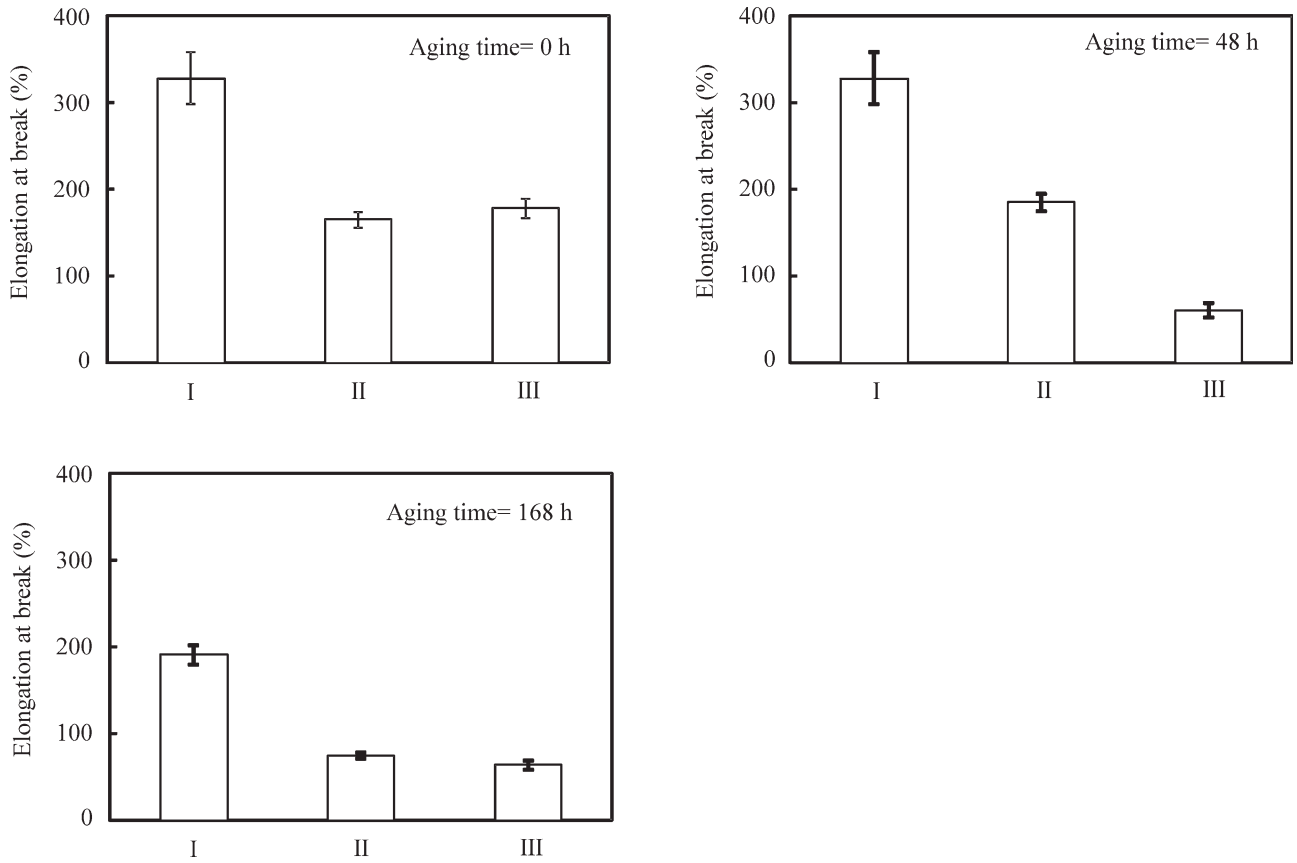

Figure 6 Comparison of elongation at breaks of samples. I: PB. II: PB(70 wt %)/FC(30 wt %). III: PB(70 wt %)/silanized FC(30 wt %) with APTMS(5 wt %). Aging temperature = r. t. (~ 20°C).

of the PB crystal phase transformation rate.[25,26] It is noted here that the order of magnitude of the water quenched samples is as follows; the PB (0.18) > the PB/FC (0.08) > the PB/silanized FC with APTMS (0.035). The order suggests that the existences of the FC and the silanized FC favor the formation of the II crystal form under the melt crystallization. The II crystal form is more stable than the I crystal one under melting state although it is less stable at r.t.[27]

Figure 9 shows the DSC curves of cooling scans for the PB, the PB/FC, and the PB/silanized FC with APTMS samples, and the crystallization temperatures (T_c) obtained are summarized in Table I. The T_c values of the PB, the PB/FC, and the PB/silanized FC are 68, 72, and 81°C, respectively. The DSC results indicate that the FC and the silanized FC become nucleating agents for the crystallization of the II crystal form. In addition, it is found that the

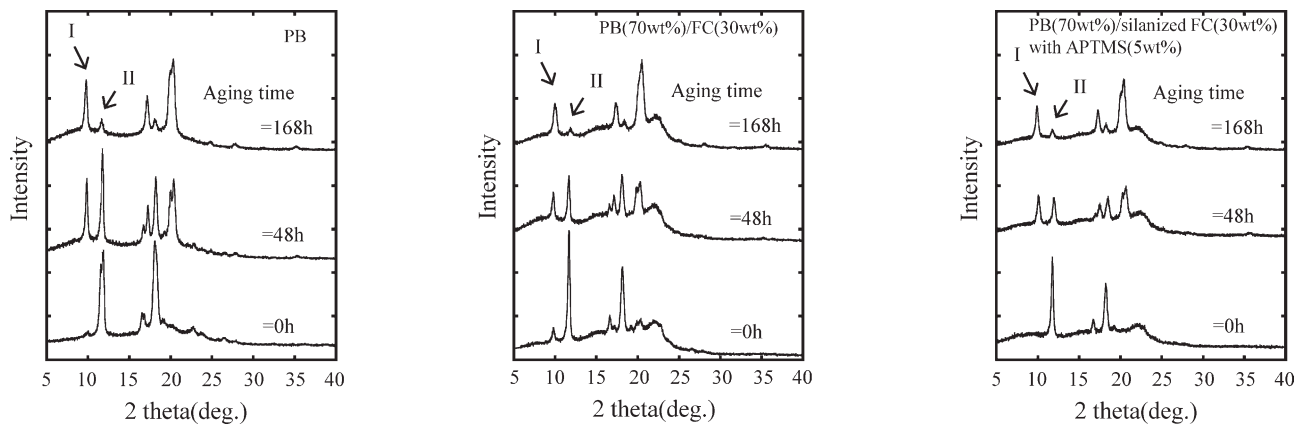

Figure 7 WAXD profiles of PB, PB (70 wt %)/FC (30 wt %), and PB (70 wt %)/silanized FC (30 wt %) with APTMS (5 wt %) at r.t. (~ 25°C).

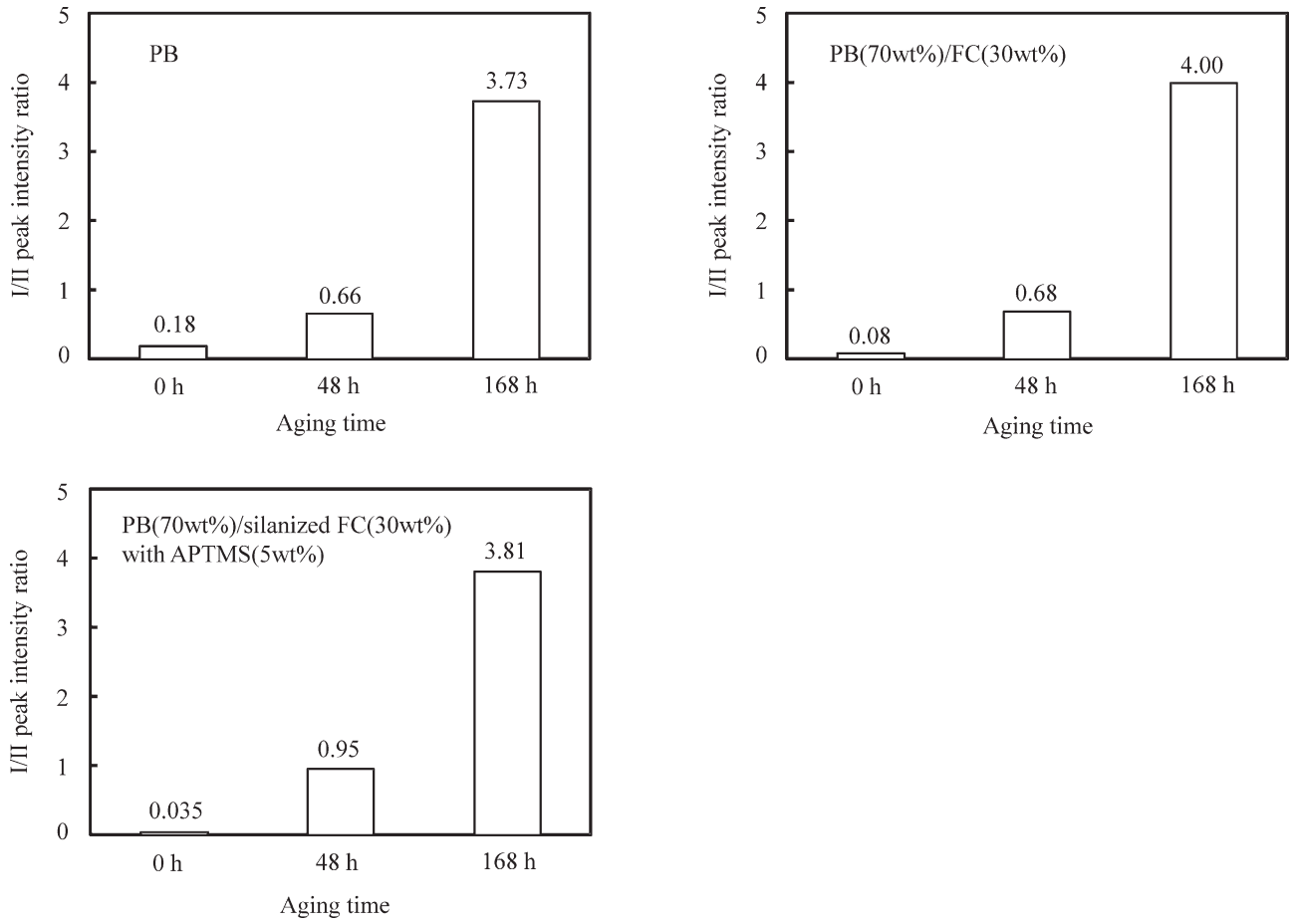

Figure 8 Changes of I/II peak intensity ratio of PB, PB (70 wt %)/FC (30 wt %), and PB(70 wt %)/silanized FC(30 wt %) with APTMS(5 wt %) at r.t. (~ 25°C).

silanized FC becomes the more excellent nucleating agent. It seems that the secondary bonding between the PB chain and the silanized FC is easily formed under the melting state and leads to the nucleation. As shown in Figure 8, the I/II peak intensity ratio is increasing with the increase in the aging time. All the samples reach the intensity ratio of ~ 4 at the 168-h aging time. In the cases of the PB and the PB/FC, the degrees of the ageing embrittlement

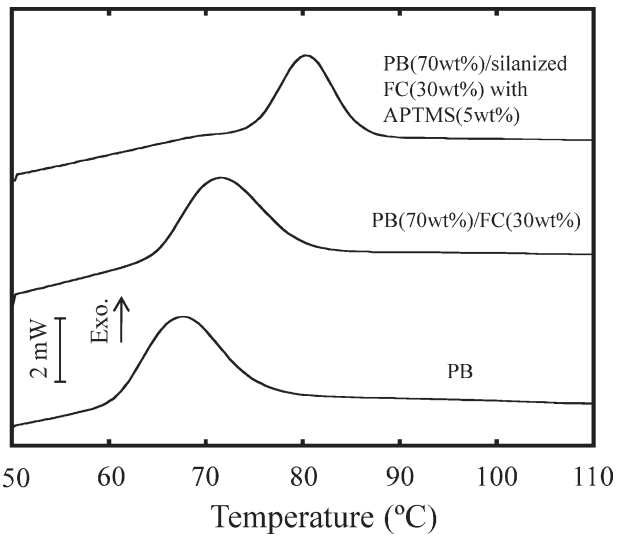

Figure 9 DSC curves of cooling scans for PB, PB(70 wt %)/FC(30 wt %), and PB(70 wt %)/silanized FC(30 wt %) with APTMS(5 wt %) samples. The exothermal peaks are corresponding to crystallization temperatures (T_c).

TABLE I
Melting Temperature (T_m) and Crystallization Temperature (T_c) of PB, PB(70 wt %)/FC(30 wt %), and PB(70 wt %)/Silanized FC(30 wt %) with APTMS(5 wt %)

Sample	Aging time (h)[a]	T_m (°C)	T_c (°C)
PB	0	122	68
PB	48	119	–
PB	168	120	–
PB/FC[b]	0	122	72
PB/FC[b]	48	120	–
PB/FC[b]	168	122	–
PB/silanized FC[c]	0	124	81
PB/silanized FC[c]	48	120	–
PB/silanized FC[c]	168	121	–

[a] Aging temperature = r.t. (ca. 20°C).
[b] PB (70 wt %)/FC (30 wt %).
[c] PB (70 wt %)/silanized FC (30 wt %) with APTMS (5 wt %).

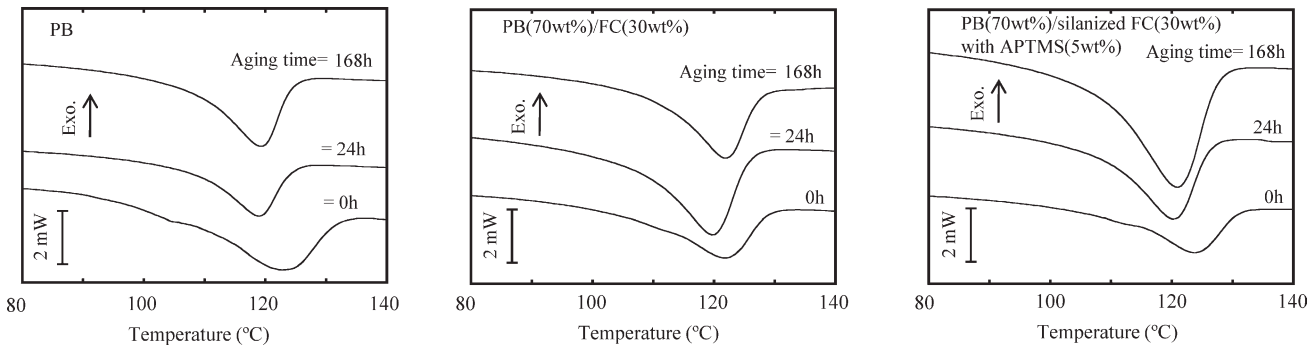

Figure 10 DSC curves of heating scans for PB, PB(70 wt %)/FC(30 wt %), and PB(70 wt %)/silanized FC(30 wt %) with APTMS(5 wt %) samples. The endothermal peaks are corresponding to melting points (T_m).

approximately consist with the magnitude of the intensity ratio. The behavior supports that these excellent ductile properties are originated from the PB crystal phase transformation. In the case of the PB/silanized FC, the change of the I/II peak intensity ratio is more rapid than the other samples at the initial stage from the 0 h to the 48-h aging time. The I/II peak intensity ratio of the PB/silanized FC reaches ~ 1 at the 48 h, and the ageing embrittlement simultaneously advances. However, as mentioned earlier, the ageing embrittlement almost stops at the 48-h aging time. It seems that an important part of the crystal playing an important role in the applied energy absorption has already been phase-transformed up to the 48-h aging time.

Figure 10 shows the DSC curves of heating scans for the PB, the PB/FC, and the PB/silanized FC with APTMS samples, and the melting points (T_m) obtained are summarized in Table I. As shown in Figure 10, the endothermal peak around T_m of the water quenched PB/silanized FC shifts to the higher temperature region when compared with those of the other samples. The T_m values of the PB, the PB/FC, and the PB/silanized FC are 122, 122, and 124°C, respectively. After the 48-h aging time, these endothermal peaks considerably shift to the lower regions, and their shapes slightly become sharp. In particular, the peak of the PB/silanized FC shifts to the much lower region. When the PB crystal phase transformation occurs, the PB lamella crystal is inevitably reorganized. These lower peak shifts are due to the lamella disorder caused by the reorganization. The thicker the lamella is, the higher the probability of containing a crystal defect to serve as a starting point of the transformation is. As mentioned earlier, the silanized FC becomes the excellent nucleating agent. Therefore, the PB/silanized FC has a greater tendency to form the thick lamella of the II crystal form than the other samples. In fact, the T_m of the PB/silanized FC is highest among these samples. The higher transformation rate of the PB/silanized FC is due to its thicker lamella. In addition, in the case of the PB/silanized FC, it seems that the fraction of the thicker lamella is considerably high, so that the lamella plays an important role in the tensile behavior. Therefore, the ageing embrittlement stops at the 48-h aging time when the thicker lamella part has been mostly transformed.

Interestingly, at the 168-h aging time, all T_m values are $\sim$ 1°C higher than those at the 48 h. These increases of the T_m values are due to an ordering of their transformed lamellae. It seems that the ordering hardly affects the tensile behavior of the PB/silanized FC, because it does not change between the 48 and the 168-h aging times.

CONCLUSIONS

In this work, the morphologies and the tensile properties of the PB, the PB/FC, and the PB/silanized FC with APTMS composites were studied. The SEM micrographs exhibited the adherent PB parts on the FC and the silanized FC, suggesting that there was a certain affinity of PB to them. It was found from the spherulite observation that the PB adsorption configuration occurred by the secondary bonding formation between the PB and the FC or the silanized FC. These tensile properties were remarkably affected by the PB crystal phase transformation. The transformation caused the ageing embrittlement of them even at r.t. In particular, the ageing embrittlement rate of the PB/silanized FC was much higher than other samples. Because the silanized FC became the excellent nucleating agent for the crystallization of the II crystal form, the PB/silanized FC was found to easily form the thicker lamella having a higher probability of containing a crystal defect to serve as a starting point of the transformation. The higher transformation rate depended on the thicker lamella formation rate and its amount.

The authors thank Japan Polychem Co. for providing the PB polymer and for partially measuring the molecular weight of the modified PB polymer.

References

1. Takase, S.; Shiraishi, N. J Appl Polym Sci 1989, 37, 645.
2. Maldas, D.; Kokta, B. V.; Daneault, C. J Appl Polym Sci 1989, 37, 751.
3. Raj, R. G.; Kokta, B. V.; Maldas, D.; Daneault, C. J Appl Polym Sci 1989, 37, 1089.
4. Hedenberg, P.; Gatenholm, P. J Appl Polym Sci 1996, 60, 2377.
5. Zhang, F.; Qiu, W.; Yang, L.; Endo, T. J Mater Chem 2002, 12, 24.
6. Qiu, W.; Zhang, F.; Endo, T.; Hirotsu, T. J Appl Polym Sci 2003, 87, 337.
7. Qiu, W.; Zhang, F.; Endo, T.; Hirotsu, T. J Appl Polym Sci 2004, 91, 1703.
8. Felix, J. M.; Gatenholm, P. J Appl Polym Sci 1991, 42, 609.
9. Qiu, W.; Zhang, F.; Endo, T.; Hirotsu, T. J Appl Polym Sci 2004, 94, 1326.
10. Hristov, V. N.; Vasileva, S. T.; Krumova, M.; Lach, R.; Michler, G. H. Polym Compos 2004, 25, 521.
11. Miyazaki, K.; Moriya, K.; Okazaki, N.; Terano, M.; Nakatani, H. J Appl Polym Sci 2009, 111, 1835.
12. Nakatani, H.; Miyazaki, K. J Appl Polym Sci 2009, 112, 3362.
13. Nakatani, H.; Hashimoto, K.; Miyazaki, K.; Terano, M. J Appl Polym Sci 2009, 113, 2022.
14. Afrifah, K. A.; Hickok, R. A.; Matuana, L. M. Compos Sci Technol 2010, 70, 167.
15. Jones, A. T. Polymer 1966, 7, 23.
16. Chau, K. W.; Yang, Y. C.; Geil, P. H. J Mater Sci 1986, 21, 3002.
17. Shieth, Y. T.; Lee, M. S.; Chen, S. A. Polymer 2001, 42, 4439.
18. Weynant, E.; Haudin, J. M.; G'Sell, C. J Mater Sci 1982, 17, 1017.
19. Felix, J. M.; Gatenholm, P. J Mater Sci 1994, 29, 3043.
20. Gray, D. G. Cellulose 2008, 15, 297.
21. Nakatani, H.; Hashimoto, K.; Miyazaki, K.; Terano, M. J Appl Polym Sci 2009, 113, 2022.
22. Nakatani, H.; Iwakura, K.; Miyazaki, K.; Okazaki, N.; Terano, M. J Appl Polym Sci 2011, 119, 1732.
23. Lenes, M.; Gregersen, O. W. Cellulose 2006, 13, 345.
24. Miyazaki, K.; Okazaki, N.; Terano, M.; Nakatani, H. J Polym Environ 2008, 16, 267.
25. Nakatani, H.; Ichizyu, T.; Miura, H.; Terano, M. Polym Int 2010, 59, 463.
26. Nakatani, H.; Ichizyu, T.; Miura, H.; Terano, M. Polym Int 2010, 59, 1673.
27. Alfonso, G. C.; Azzurri, F.; Castellano, M. J Therm Anal Cal 2001, 66, 197.